Journal of Sound and Vibration (2000) **232**(5), 839–856
doi:10.1006/jsvi.1999.2248, available online at http://www.idealibrary.com on IDEAL®

A STANDING-WAVE-TYPE SLOSHING ABSORBER TO CONTROL TRANSIENT OSCILLATIONS

J. G. Anderson, S. E. Semercigil and Ö. F. Turan

Faculty of Engineering and Science (*Mechanical Engineering*), *Victoria University of Technology*, *Footscray Campus*, *P.O. Box* 14428 *MCMC*, *Melbourne*, *Victoria* 8001, *Australia*

(*Received* 6 *August* 1998, *and in final form* 5 *March* 1999)

The primary purpose of this study is to introduce a sloshing absorber as a practical alternative to the damped tuned absorber. In addition, a numerical simulation procedure is introduced as a computer-aided design tool. The problem of interest is the control of excessive oscillations of a mechanical oscillator in response to an initial displacement. Tuned vibration absorbers are frequently used for this purpose, and if damping is included in the tuned absorber, control action is quite effective. The problem, however, is that inclusion of an energy dissipation element necessitates frequent maintenance in practice. The suggested control technique here is a sloshing absorber, in place of the damped tuned vibration absorber. In contrast to a tuned absorber, a sloshing absorber accomplishes energy dissipation through sloshing. Therefore, it may be virtually maintenance free. Also for practical applications, this type of absorber can be an advantage where existing water storage tanks can be modified to control vibrations of the supporting structure.

1. INTRODUCTION

Numerical simulations and experimental observations are presented in this paper to compare the performances of a sloshing absorber and a conventional tuned absorber in controlling excessive transient vibrations of a resonant structure. A tuned absorber is a mechanical oscillator whose resonance frequency is tunded at a critical frequency of the structure to be controlled. Comprehensive treatment of this classical subject may be found in the standard textbooks such as Hunt [1] and Snowdon [2]. Figure 1 schematically illustrates such a system. The primary system with mass m_1, damping c_1 and stiffness k_1 represents the structure to be controlled, whereas the auxiliary oscillator with m_2, c_2 and k_2 is the tuned absorber. Tuning is usually accomplished by designing the natural frequency of the absorber to be the same as the structure to be controlled: $(k_1/m_1)^{1/2} = (k_2/m_2)^{1/2}$. Some slight deviations from this basic relationship may occur when using significant values of c_2.

With an undamped tuned absorber, control may be very effective when the structure to be controlled is excited harmonically at the tuning frequency. However, this effectiveness deteriorates drastically in the case of transient disturbances. In transient cases, the oscillatory energy may be transferred readily to the absorber due to strong interaction. However, this energy returns to the structure resulting in a poor control action, unless some means of energy dissipation is provided in the absorber. A damper, c_2, may be included in the absorber to improve performance. Optimum values of damping are derived in reference [2]. Inclusion of a damper, however, presents problems of frequent maintenance and reduces the practical value of the controller. A sloshing absorber may be a simple alternative to the conventional tuned absorber to avoid such problems.

0022-460X/00/200839 + 18 $35.00

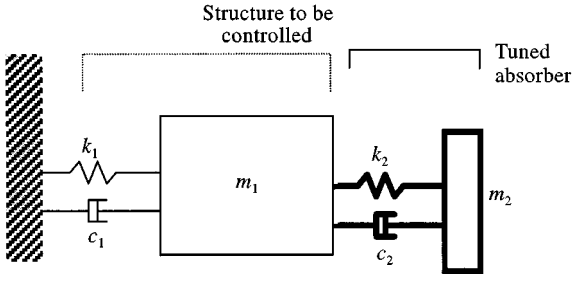

Figure 1. A tuned vibration absorber and the structure to be controlled.

Sloshing refers to low-frequency oscillations of a liquid in a container. Transportation of liquid cargo, earthquake-induced sloshing in storage tanks and fuel tanks of aircraft and aerospace vehicles, are some of the common engineering applications where sloshing occurs. In these applications, liquid sloshing needs to be suppressed, because the dynamic behaviour of the sloshing liquid affects the stability of the container or the manoeuvrability of the transportation vehicle. Hayama and Iwabuchi [3] suggested an inverted U-tube to suppress sloshing. Muto *et al.* [4] used strategically placed submerged blocks and plates in the container. Hara and Shibata [5] used an active control approach. They injected air bubbles, critically timed to cause enough momentum opposition between the rising sloshing wave and that of the injected bubbles to suppress sloshing. Floating and submerged dumb-bell controllers have also been reported as effective controllers in cylindrical containers in references [6, 7].

Most of the earlier work in the field of sloshing has been directed to understanding the physics of the phenomenon for the purposes of suppressing it. The objective in this study is to intentionally induce sloshing of a liquid in a container which is in turn attached onto a resonant structure. In such a configuration, fluid forces may be used to counteract and suppress structural oscillations. The proposed sloshing absorber is shown in Figure 2, when attached on the same structure as in Figure 1. Therefore, the principle of this particular structural control technique is similar to that of a classical tuned vibration absorber. However, a distinct potential advantage of the proposed approach is that existing liquid storage tanks may be employed for structural control purposes. For cases where the sloshing controller is an added component to reduce structural oscillations, its inherent characteristic of requiring virtually no maintenance is a significant practical advantage.

The concept of using sloshing forces for structural control has been suggested earlier. Fujii *et al.* [8] reported using liquid motion in a circular container to reduce wind-induced oscillations at Nagasaki Airport Tower and Yokohama Marine Tower to about half of the uncontrolled values. Abe *et al.* [9] reported effective control using a U-tube with a variable orifice passage. Modi and Welt [10] poineered research on Nutation Dampers and their applications in practical structures. In a later work, Seto and Modi [11] presented work to use fluid–structure interaction to control wind-induced instabilities. In sloshing controllers, plain water is usually used as the working fluid which has poor energy dissipation characteristics. To improve dissipation, Kneko and Yoshida [12] suggested employing a net to obstruct the flow of liquid during sloshing, and reported optimum levels of obstruction for best structural control.

The earlier work invariably dealt with shallow liquid levels in the tuned sloshing absorbers. Even in Kaneko and Yoshida [12], which employs a relatively larger depth than those of the others, the water depth is approximately equal to 35% of the length of the container. Such small depth may be quite limiting for some geometries such as liquid

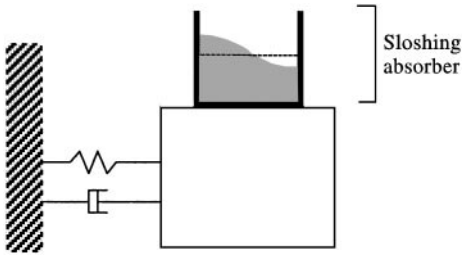

Figure 2. The proposed sloshing absorber attached on the structure to be controlled.

storage tanks in tall structures. This particular point is addressed in this study with water depth of the absorber comparable to the length of the container.

Shallow liquid levels in a container are likely to induce travelling sloshing waves, whereas deeper liquid levels cause a standing sloshing wave in the fundamental mode. Without additional measures, the suppression effect of a standing sloshing wave is quite limited. For such cases, the oscillatory energy of the structure could be easily transferred to the sloshing liquid, if there is a strong interaction. A strong interaction is assured when the sloshing frequency is close to the natural frequency of the structure. However, if there is no dissipative mechanism in the container, this transferred energy in the liquid may travel back to the structure to excite it quite easily. Oscillation of energy between the structure and the liquid produces a beating envelope of oscillations of the structure. Such a beat drastically reduces the control effect, which is discussed in more detail later in this paper [12, 13].

To improve the performance of the standing wave sloshing absorber, fixed plate baffles are employed in the liquid container. Similar baffles were investigated earlier by Muto *et al.* [4] where the purpose was to suppress the liquid sloshing when the liquid container was excited by external means. An earlier study of the authors also demonstrated the effectiveness of this particular geometry to suppress sloshing [7]. As an extension of this earlier work, now baffle plates are used to modify the characteristics of the sloshing absorber to improve the control of structural oscillations.

2. RESPONSE OF TUNED VIBRATION ABSORBER

Histories of the displacement of m_1 and the control force of the tuned absorber on m_1, are shown in Figure 3, after an initial displacement of 1·3 mm. The horizontal axis represents non-dimensional time, t/T_0, where T_0 is the natural period of the structure to be controlled alone. The control force is comprised of the spring force and the damper force of the tuned absorber. The solution was obtained by numerically integrating the coupled system of differential equations using a standard fourth order Runge–Kutta procedure. The time-step was taken to be smaller than 1/40th of the shortest expected period of oscillations. Details of such a procedure can be found in standard textbooks on vibration theory [15]. System parameters are summarized in Table 1 for reference. The structure to be controlled is undamped, $c_1 = 0$. In Figure 3(a), the absorber is undamped, whereas in Figures 3(b)–(d) the value of ξ_2 is 0·025, 0·19 and 1·24. Here, the critical damping ratio of the absorber ξ_2 is defined as $\xi_2 = c_2/[2(m_2 k_2)^{1/2}]$. In Figure 3(a), when the tuned absorber is undamped, the oscillatory energy periodically travels back and forth between the structure to be controlled and the absorber. Due to this strong interaction, which is the result of tuning the absorber at the natural frequency of the structure, an initial displacement of 1·3 mm rapidly

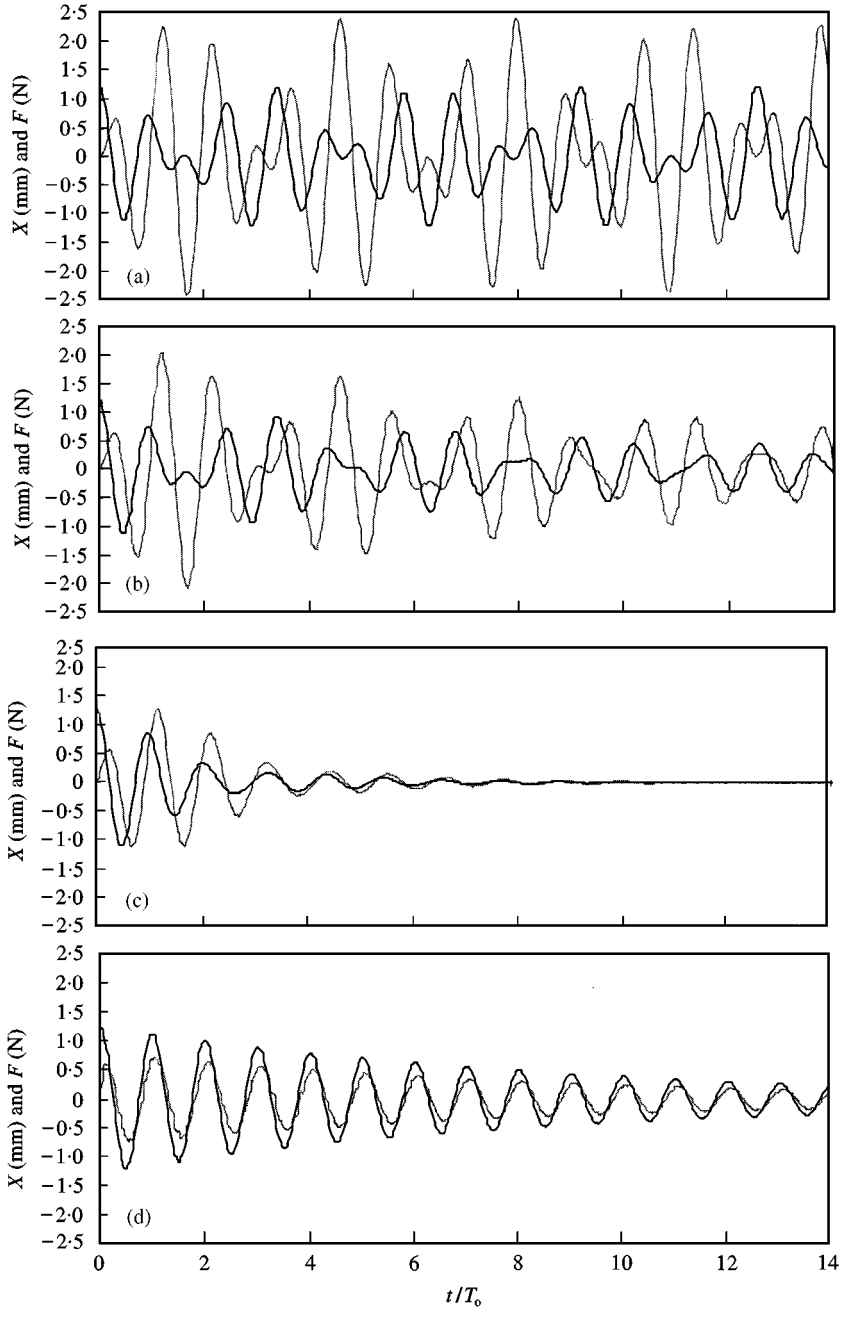

Figure 3. Displacement —— and force —— histories of the tuned absorber for (a) $_{.2} = 0$, (b) $_{.2} = 0{\cdot}025$, (c) $_{.2} = 0{\cdot}19$ and (d) $_{.2} = 1{\cdot}24$, respectively.

decays to very small values around 1·8 periods. At this instant, the absorber oscillates quite violently as indicated by the control force. Starting from about two natural periods, however, the structure receives the absorber's energy back, resulting in as large displacements as its initial displacement. This periodic exchange of energy produces periodic beats of the envelopes of both displacement and force oscillations. The beat of the

TABLE 1

System parameters. In each column, experimental/computational values are given when they differ. f_n and ξ_{eq} represent the fundamental frequency and the equivalent viscous damping ratio

	Mass (kg)	Stiffness (N/m)	f_n (Hz)	ξ_{eq}
Structure	27·9/**28**	5826/**6374**	2·6 ± 0·2/**2·4**	0·004 ± 0·002
Tuned absorber	2·8	579·45	2·3	
Water	2·8		2·3 ± 0·2/**2·2**	

two histories are almost perfectly out of phase, indicating where most of the oscillatory energy is at a particular time.

In Figure 3(b), some light damping, $\xi_2 = 0{\cdot}025$, is included in the tuned absorber producing a significant difference from the results in Figure 3(a). The strong interaction and the resulting beat are still quite clear in Figure 3(b). However, the peak amplitudes decay gradually as a result of energy dissipated through ξ_2. When ξ_2 is increased to 0·19 in Figure 3(c), the beat disappears completely leaving a very effective control action. Oscillations virtually stop after eight periods. In Figure 3(d), when ξ_2 is 1·24, the effective control in Figure 3(c) deteriorates quite drastically. Due to having too large a resistance between the oscillator and the absorber, the absorber is no longer able to oscillate freely with respect to the structure to be controlled. The limited relative motion still dissipates some energy resulting in a slow rate of decay of the oscillation envelope. Any further increase in the value of ξ_2 would worsen the situation, eventually locking m_2 on m_1 and reverting to an undamped oscillator.

Hence, the conventional tuned absorber is certainly capable of producing effective control action for a value of ξ_2 around 0·19. This ξ_2 is in close agreement with the optimum value suggested in reference [2]. For such optimally damped cases, the control is so effective that the total energy of the system is dissipated within eight periods after the initial disturbance. Such tuned absorbers have been used in towers and bridges [16]. The viscous damping is introduced using hydraulic mechanisms which are rather complex and demand continual maintenance. Avoiding such a need for maintenance should certainly be an advantage in application. The sloshing absorber discussed in the next section is proposed to gain such an advantage.

3. SLOSHING ABSORBER

Examination of the response with the sloshing absorber as shown in Figure 2 consisted of attaching the liquid container onto the oscillator at first. The baffle plates were added to the container to improve the control performance. In this section, the experimental procedure will be outlined first. Then the numerical model will be described before the results are discussed. Several different baffle configurations were simulated with the suggested sloshing absorber. Baffle configurations were evaluated numerically to be verified experimentally. Results presented here are those which produced the best control effect on the structure.

3.1. EXPERIMENTS

The sloshing absorber consisted of a rectangular container of 130 mm length by 210 mm width, filled with water to a depth of 100 m corresponding to a mass of approximately

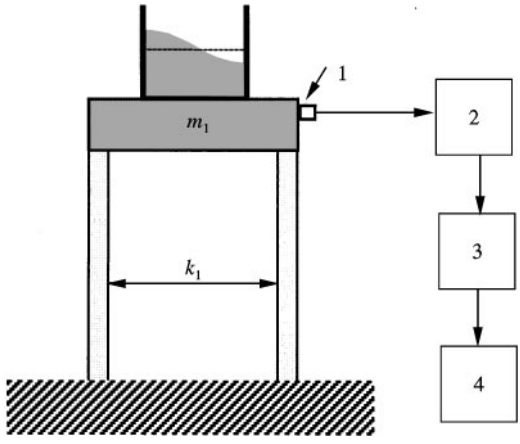

Figure 4. Experimental set-up. 1: Keyence, LB-12 laser displacement transducer; 2: Keyence LB-72 amplifier and DC power supply; 3: DataAcq A/D conversion broad; 4: Total Peripherals Group, Pentium 200 MHz, Personal Computer.

2·8 kg. The structure consisted of a mass of 27·9 kg supported on four 390 mm long mild steel columns of 3·5 mm thickness and 22 mm width. The ratio of the mass of water in the container to the mass of the structure was 10%. The structure exhibited light damping under free vibrations and had a natural frequency of $2{\cdot}3 \pm 0{\cdot}2$ Hz. The fundamental sloshing frequency of the liquid in the container was $2{\cdot}3 \pm 0{\cdot}2$ Hz. The width of the container was large enough to allow a virtually two-dimensional standing sloshing wave along the width of the container. System parameters are summarized in Table 1.

For each test case, the structure was displaced by $1{\cdot}30 \pm 0{\cdot}05$ mm before being released to oscillate freely. The displcement of the structure was tracked with a laser displacement transducer and then recorded. The experimental set-up is shown schematically in Figure 4.

After determining the behaviour of the free vibrations of the structure alone, the rectangular container was secured to the structure. A series of tests was performed where the liquid motion was controlled by contilevered baffles attached to the vertical sides of the container. The baffles were constructed from 3 mm thick plywood, and their surfaces were sealed to reduce water absorption. The performance of the damper has been evaluated for a baffle size of 10 mm located at different distances from the liquid surface.

3.2. NUMERICAL MODEL

A two-dimensional numerical model of the rectangular container was created using CFX version 4·1 [17]. For liquid sloshing, a two-phase model was adopted because of the presence of a liquid–gas interface at the free surface. The Navier–Stokes equations were solved using the Volume of Fluid method. Each phase was assumed to be homogeneous, and a clear definition of the liquid-free surface was obtained by using a surface sharpening algorithm. Surface tension was not included, and no-slip condition was imposed at solid boundaries. A mass source tolerance of 10^{-6} was used to judge convergence in single precision. The maximum number of iterations was set to be 50 per time step at each cell.

Grid independence was achieved after evaluating a series of mesh refinements. A non-uniform grid of 64×70 cells was chosen for the simulations. This grid is shown in Figure 5. The resolution of the grid was finer in the region near the baffles to increase the

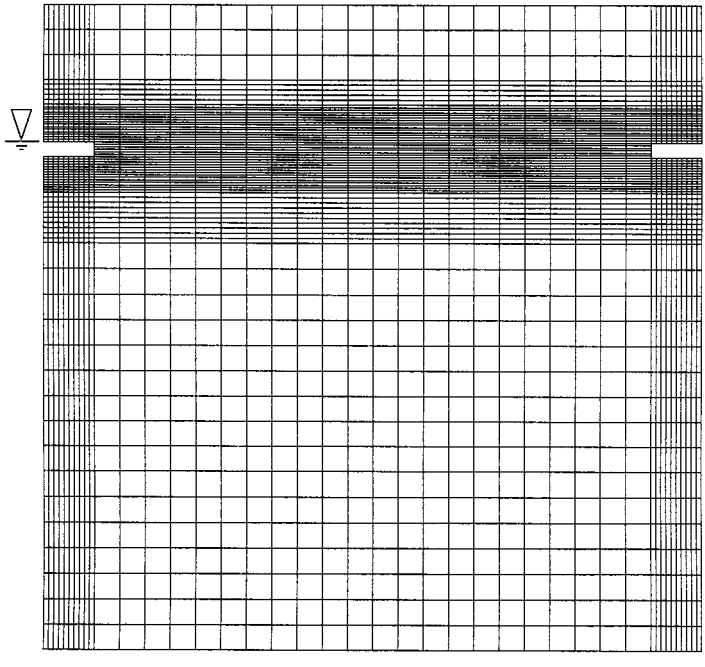

Figure 5. Numerical grid of the container showing 10 mm long cantilevered baffles located on the static liquid surface.

accuracy of the predictions. A time-step of 0·001 s was determined to be the largest possible time-step for accurate numerical prediction.

The equation of motion of the structure in Figure 2 was solved at each time step in a FORTRAN routine developed within the CFX environment. The force of the sloshing absorber on the structure was obtained by integrating the pressure distribution on the walls of the sloshing absorber. The effect of the sloshing force on the displacement of the structure was then determined. This displacement then provided the next boundary condition for the sloshing absorber.

The mass, m, of the oscillator was set to 30·8 kg (consisting of 28 kg mass of the structure and 2·8 kg mass of the water). The stiffness, k, of the spring was 6374 N/m. Structural damping was set to zero. Parameters of the numerical model corresponding to that of the experiments are listed in Table 1. The force of liquid sloshing on the structure was determined by calculating the resultant pressure force on the walls of the container.

3.3. RESULTS

Initial numerical predictions were performed to determine the strongest interaction between the structure and the liquid. This "tuning" was obtained for a frequency ratio of 0·95. This value represents the ratio of the fundamental sloshing frequency (when the container is alone), to the structural natural frequency (including the added liquid mass). This frequency ratio agrees with those in references [3, 8].

In Figures 6(a–d), the numerically predicted and experimentally observed displacement histories of the oscillator are given along with the numerically predicted sloshing force on the oscillator. Again, the time is non-dimensionalized by dividing with the period of the

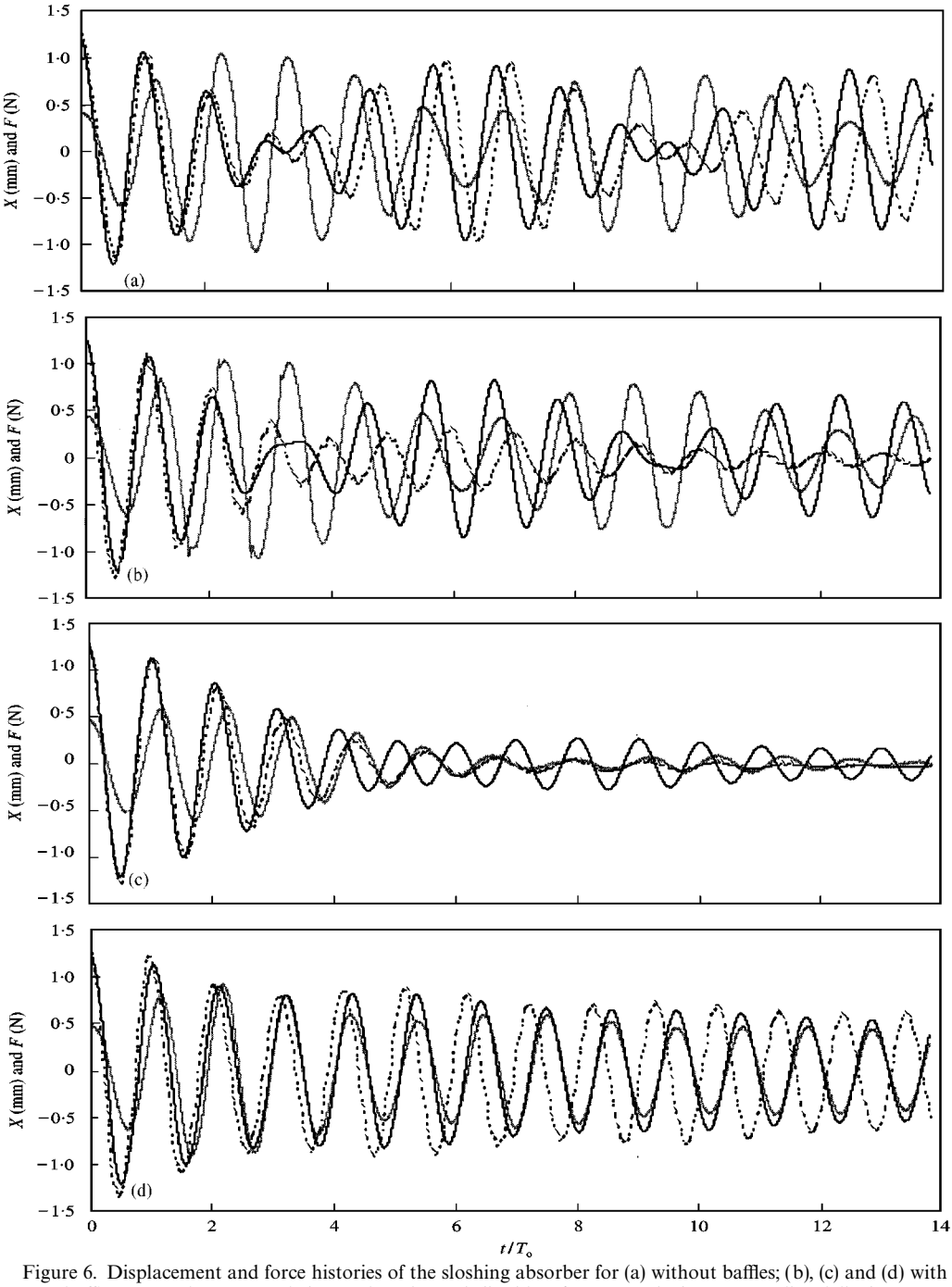

Figure 6. Displacement and force histories of the sloshing absorber for (a) without baffles; (b), (c) and (d) with 10 mm baffles, 5 mm above, 5 mm below and on the static liquid surface respectively. ——, predicted displacement; ....., experimental displacement; —, predicted sloshing force.

oscillator alone. The displacement history of the oscillator starts with an initial displacement of 1·3 mm. At the start, the total energy of the combined system is the potential energy stored in the spring of the oscillator due to its initial displacement. Numerical predictions will be discussed first.

In Figure 6(a), after the oscillator is released from 1·3 mm, its amplitude decays while the amplitude of the sloshing force increases as the sloshing motion develops. After approximately 3·5 natural periods, the displacement experiences its smallest amplitude, whereas the sloshing force is at its largest value. This phenomenon indicates an exchange of energy between the oscillator and the sloshing liquid. In contrast to the situation at the start, now most of the energy is with the sloshing liquid. This exchange continues as the energy is transferred back to the oscillator, around 6·3 periods, and back to the liquid, around 9 periods, forming a "beat" envelope of oscillations.

Strong interaction of oscillator is desirable with the sloshing liquid during the initial stages. This strong interaction assures that the oscillatory energy is taken away from the structure to be controlled. However, as mentioned earlier, the liquid level used in this study results in a standing sloshing wave which has no effective means of dissipating energy. Hence, the oscillatory energy eventually returns to the oscillator producing a very poor control effect. Some additional means of energy dissipation during sloshing must be introduced to improve control.

In Figures 6(a–d), histories of the same three parameters are shown as in Figure 6(a). However, in these three frames, there are two baffle plates cantilevered symmetrically from opposite sides of the container. These plates are all 10 mm long and 3 mm thick. In Figure 6(b), the baffles are located 5 mm above the static free surface of the liquid, in Figure 6(c) they are submerged 5 mm below the surface and in Figure 6(d) the baffles are on the surface. In Figure 6(b), when the baffle plates are 5 mm above the surface, the response of the system is identical to that of no baffles in Figure 6(a), until the surface wave reaches a height of 5 mm. This instant is clearly signified around 1·8 periods where the sloshing force displays some discontinuity. The overall difference between Figures 6(a, b), however, is quite insignificant. This relative ineffectiveness could be attributed to minimal interaction between the surface of the liquid and the baffle plates since the liquid surface is free from contact with the baffles during most of its cycle.

The best control effect is obtained for the case shown in Figure 6(c) when the baffles are 5 mm below the surface. For this case, the disturbance in the flow is able to allow a relatively strong interaction at the start. After the initial strong interaction, however, the sloshing liquid is disturbed enough so that the beat in the envelope of structural oscillations is much less pronounced. In addition, the structural displacements are smaller than 0·25 mm (about one-fifth of the initial displacement) after approximately five natural periods, whereas peak displacements reach up to 1·0 mm for the case in Figure 6(a).

In Figure 6(d), when the baffles are on the surface, the beat shown in the preceding frames disappears completely. The sloshing force oscillates in almost perfect phase with the oscillator. This in-phase motion between the sloshing liquid and the oscillator, prevents the transfer of energy from the oscillator to the liquid as they move in unison. Therefore, surface baffles modify the sloshing wave too strongly resulting in a poor control action.

In all four frames of Figure 6, the experimentally measured displacement of the oscillator is also given for comparison purposes. These experimentally measured displacements follow the same trends as those of the numerical predictions. However, the experimental frequency of oscillations is about 5% smaller in Figure 6(a) and 5% higher in Figures 6(b–d) than the numerical one. In addition, especially for the two more effective cases in Figures 6(b, c), when the baffles are 5 mm above and below the surface, the experimentally observed control of the structure is more effective than predicted. This pronounced effectiveness may be attributed to the dissipation of energy due to surface roughness and surface tension effects and light structural damping which are not included in the numerical model. For the case when the buffles are at the surface in Figure 6(d), the experimentally measured displacements have just as ineffective a control as the numerical predictions, due to the

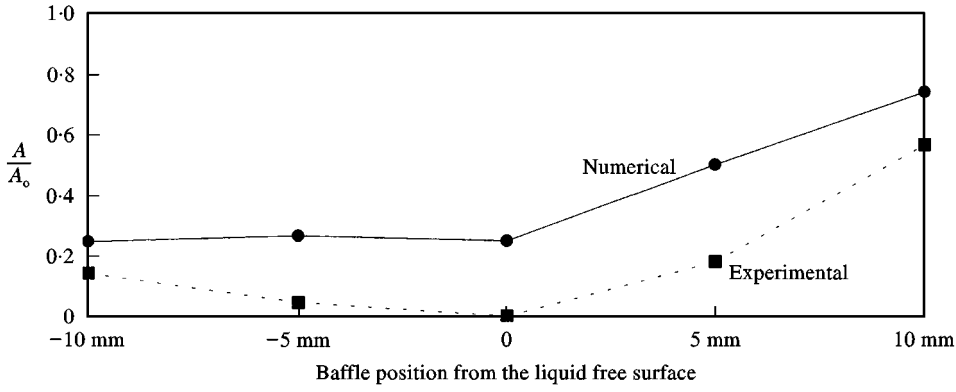

Figure 7. Non-dimensional sloshing amplitude plotted against baffle position.

in-phase motion discussed earlier. Even with the differences, the comparisons clearly indicate that the numerical predictions are able to capture the significant trends in the control action. The predicted control may be conservative, assuring that the control may well be better in application. Hence, the numerical model is certainly a useful tool to predict performance and select the promising configurations for practical applications.

The trends observed in Figure 6, where the baffle plates are positioned at different locations from the surface of the liquid, may be explained in relation to the information presented in Figure 7. The results in Figure 7 correspond to the case where the same container was excited sinusoidally at the fundamental frequency with a peak-to-peak amplitude of 2·5 mm. The horizontal axis of Figure 7 shows the position of the baffles at 5 mm intervals from 10 mm under the surface to 10 mm above the surface. The numerical predictions are marked with (●), whereas (■)'s indicate the corresponding experimental observations. The vertical axis represents the ratio, A/A_0, of the amplitude of the sloshing wave with, A, and without, A_0, a baffle. Hence, any reduction in the sloshing amplitude is reflected with ratio smaller than 1·0.

Numerical predictions consistently indicate at least a 75% reduction for all locations up to the liquid surface. Then the reduction effect deteriorates almost proportionally with the distance the baffles are placed away from the surface. As before, experiments (■) show consistently more effective control than what could be predicted (●) for all cases. As before, this difference is again attributed to the surface tension and surface roughness effects which were not modelled in the numerical simulations. When the baffles are at the surface, no measureable amplitude could be observed experimentally, resulting in perfect control. For this case, the liquid acted as if it was just an added mass in the container moving in perfect phase with it. For the results presented in Figure 6(d), when the same container was attached as the controller on the oscillator, the same overly suppressed sloshing wave was observed which prevented the transfer of energy from the oscillator. As a result of this too effective sloshing control, the sloshing controller behaved similarly to that in Figure 3(d) when the absorber was overdamped.

In Figures 8 and 9, force versus displacement phase plots are given of the tuned absorber and sloshing absorber respectively. The diamond-shaped phase pattern of the undampled tuned absorber in Figure 8(a) is also barely noticeable in that of the sloshing absorber in Figure 9(a). The trace of force–displacement is characterized by a series of ellipses formed either in counter-clockwise or in clockwise directions. By changing the rotation direction, the ellipses cross over one another creating many intersections, representing a poor control action. In the sloshing absorber, a small amount of energy is dissipated through viscosity of

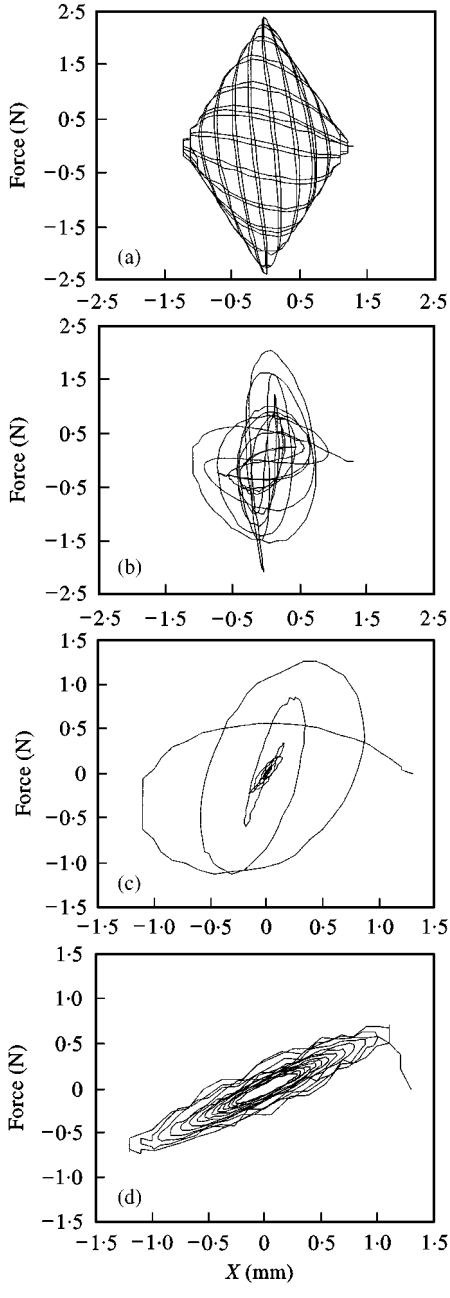

Figure 8. Force–displacement phase plots of the same cases as in Figure 3.

the fluid. Figure 9(b) shows that the performance of the sloshing absorber shown in Figure 8(b). The optimal cases of both absorbers are given in Figures 8(c) and 9(c). These phase plots have a distinct counter-clockwise pattern that forms a spiral towards the origin. As indicated by a comparison of Figure 9(d) with Figure 8(d), the surface baffles make the sloshing absorber behave like an overdamped tuned absorber. A minimal elliptical area is enclosed for each cycle of oscillations, the slope of the longer axes of the ellipse indicating

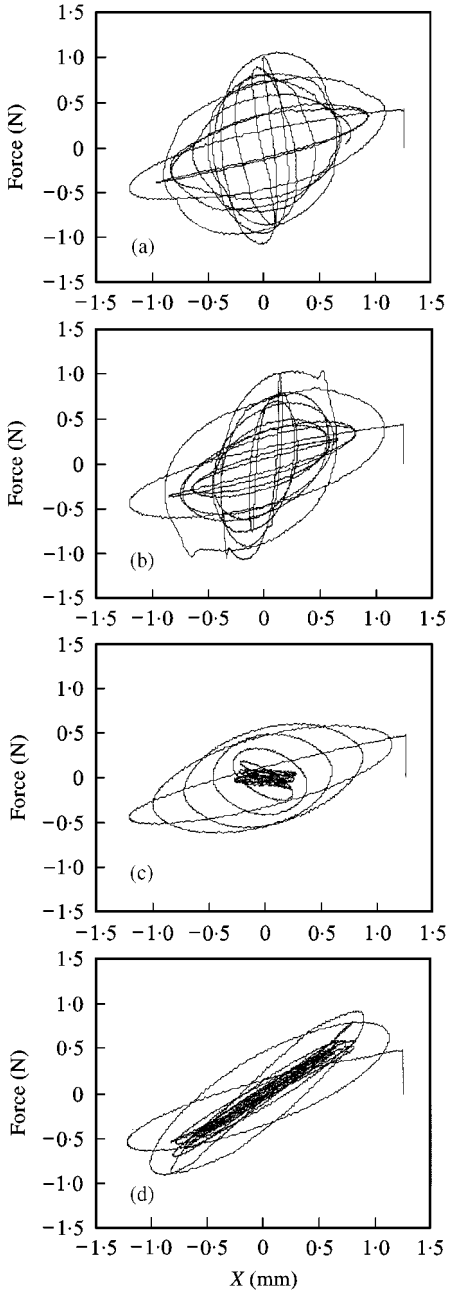

Figure 9. Force–displacement phase plots of the same cases as in Figure 4.

the stiffness of the oscillator. For the tuned absorber, the ellipses are concentric with a constant slope. However, for the sloshing absorber, the slope changes due to the non-linear nature of liquid sloshing.

Histories of the transient energy of the oscillator are shown for the same undamped, lightly damped, optimally damped and the overdamped cases from frame (a) to frame (d) in Figures 10 and 11 for the tuned and the sloshing absorbers respectively. These histories are

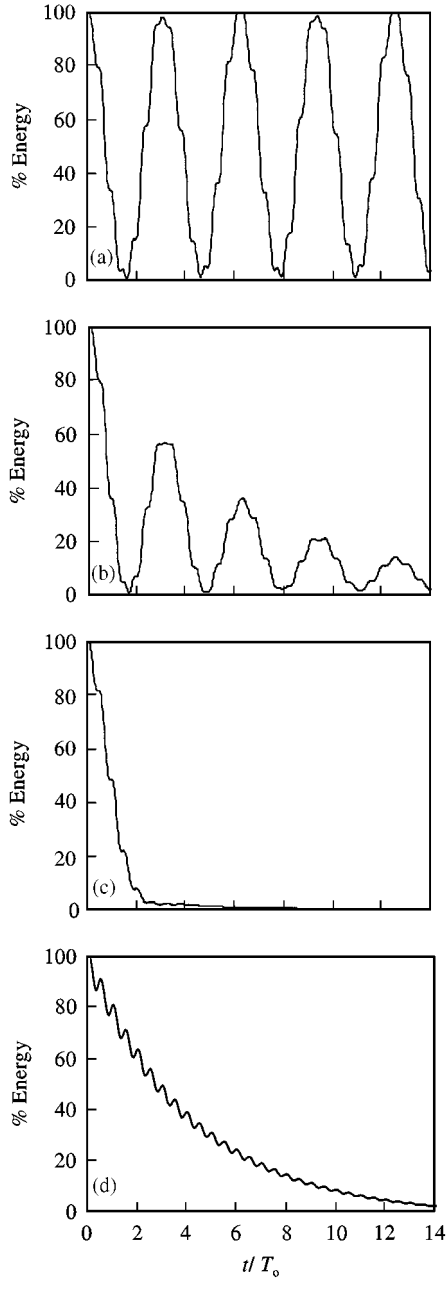

Figure 10. % Energy of the structure plotted against non-dimensional time for the same cases as in Figure 8.

obtained from the product of the velocity of the oscillator and the control force. Figure 10(a) has large fluctuations of energy due to the strong beat. In Figure 10(b), there is some dissipation due to light damping. However, beat instances are clearly marked as the oscillatory energy is exchanged between the structure and the tuned absorber. Figure 10(c) corresponds to the optimal damping with a steep slope of decay and no beat. The

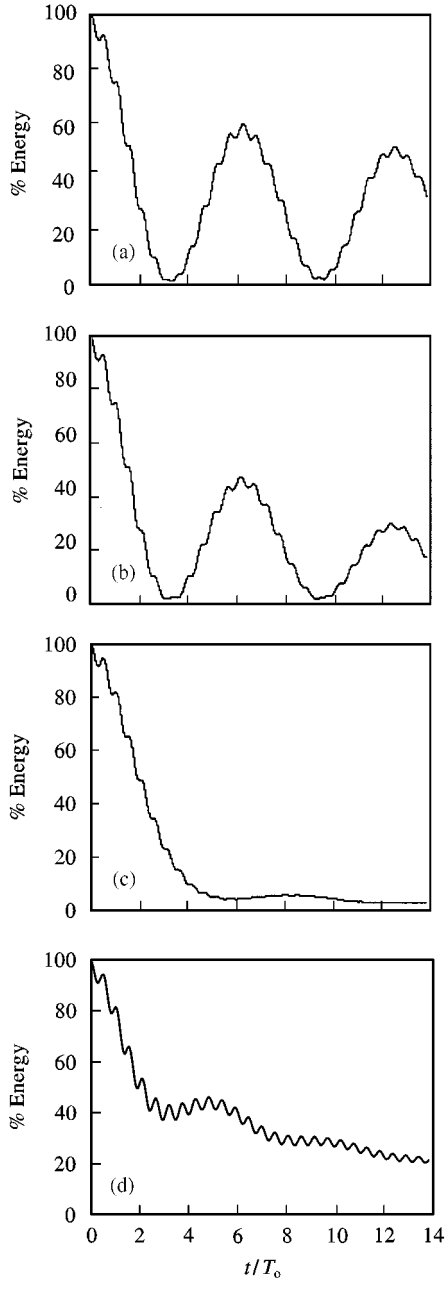

Figure 11. % Energy of the structure plotted against non-dimensional time for the same cases as in Figure 9.

overdamped tuned absorber results in poor interaction between the structure and the absorber as shown in Figure 10(d). Hence, the energy dissipation rate is small.

In Figure 11, similar comments are valid for the sloshing absorber as those for the tuned absorber. In Figure 10(a) with no baffles, however, the beat period is approximately twice as long and there is some energy loss due to the viscosity of the sloshing liquid. In Figure 11(b), energy dissipation rate is marginally enhanced with the beat still clearly apparent when the

baffles are 5 mm above the free surface. The most effective dissipation of energy corresponds to the case in Figure 11(c) where the baffle plates are 5 mm under the surface. In Figure 11(d), sloshing wave is suppressed too effectively with the surface baffles resulting in poor energy exchange and poor rate of energy dissipation.

4. ON PRACTICAL APPLICATION

In cases where full-scale experiments are expensive or dangerous, it can be an advantage to use scaled experiments and numerical predictions to determine potentially promising solutions. Here, scaling is applied to the entire absorber–oscillator system. Therefore, the promising results of the simulations presented earlier can be scaled to systems of any practical size, without having to perform new simulations.

Like many other phenomena involving liquids with free surfaces, liquid sloshing can be scaled using Froude, Reynolds and Euler numbers. Bass *et al.* [17] used Froude and Euler scaling to conduct experiments for liquid sloshing of 1/30th to 1/50th size of prototype tanks containing liquefied natural gas. Muto *et al.* [4] also used Froude scaling to represent liquid sloshing in a prototype tank with a 1/30th scale model using water as the working fluid. The difference between the present work and the earlier applications, is that here the displacement of the system container is governed by significant fluid–oscillator interaction, and there is strong interaction between the sloshing liquid and baffle plates. In this section, the scaling parameters developed for a sloshing absorber coupled with the oscillator are given. Froude number is used to scale displacement and time. Reynolds and Euler numbers are used to scale viscosity and pressure force respectively.

Scaling starts by selecting a geometric scale $\alpha = L_m/L_p$ where L_m and L_p are the model and prototype lengths respectively. All dimensions of the absorber have this geometric scale between the model and prototype systems. The mass ratio of the liquid to the oscillator is kept constant. Having selected α, the mass of the liquid in the scaled absorber can be calculated by maintaining $\rho_m = \rho_p$ where ρ is the liquid density. After determining the dimensions of the prototype absorber, Froude scaling is used for displacement and time scaling. Froude number is the ratio of inertial to gravity forces for flows with free surfaces and is defined as

$$Fr = \frac{V^2}{gX}, \tag{1}$$

where X is the displacement, V the velocity of the coupled absorber–oscillator system and g the gravitational acceleration. For a model wave scale to a prototype wave, Froude scaling results in the following relationships for velocity V, displacement X and time T:

$$V_m = V_p\sqrt{\alpha},$$

$$X_m = X_p\alpha,$$

$$T_m = T_p\sqrt{\alpha}. \tag{2}$$

Here, the relationship for T is used to scale the period of structural oscillations as well as the period of sloshing in the absorber. This expression governing T can also be obtained using the Strouhal number, $St = \omega L/\sqrt{gl}$ where ω is the sloshing frequency and L is the container length.

Reynolds number, *Re*, is the ratio of inertial to viscous forces, and is used here to scale vicsous effects. For liquid sloshing, Reynolds number is defined as

$$Re = \frac{\rho L\sqrt{gL}}{\mu}, \tag{3}$$

where μ, ρ and L are absolute viscosity, density and length of the container in the direction of liquid sloshing respectively. If viscous effects are important, then *Re* is kept constant by scaling viscosity for $\rho_m = \rho_p$. Bass *et al.* [17] reported that for sloshing in tanks containing liquefied natural gas, viscous effects were insignificant if *Re* number was larger than 10^3, and for such cases, viscous scaling need not be considered. Therefore, the liquid in the model absorber need only have the same density as the liquid in the prototype and a viscosity low enough to give a Reynolds number of greater than 10^3. This conclusion is in close agreement with observations given by Popov *et al.* [18] for liquid sloshing in horizontal cylindrical road containers. Popov *et al.* showed viscosity had no effect for *Re* in the range 10^5–10^7, and the effect was small for *Re* in the range 10^3–10^5. If however, Reynolds number in the prototype absorber is less than 10^3, viscosity will have some effect on liquid sloshing and scaling of viscosity may be important.

Euler number, *Eu*, is the ratio of pressure to inertial forces, and has been used here to scale sloshing impact pressures on the walls of the absorber as follows:

$$Eu = \frac{p}{\rho V^2}. \tag{4}$$

Substituting $V_m = \mathrm{V}_p\sqrt{\alpha}$ from equation (2) gives

$$\frac{p_m}{p_p} = \alpha\frac{\rho_m}{\rho_p}. \tag{5}$$

Since pressure is the distributed load per unit area.

$$\frac{F_m}{F_p} = \alpha^3 \tag{6}$$

for $\rho_m = \rho_p$, where F is the pressure force which is the control force on the oscillator. Using this relationship, the force amplitude for the prototype system can be determined from that of the model system, where time is scaled using equation (2).

As an example, the model used for the analysis presented in the earlier sections of this paper was scaled to a larger prototype system, using $\alpha = 0{\cdot}026$. This geometric scale value was chosen to give absorber dimensions of 5000 mm length and 8100 mm width, containing 158,427 kg of water representing a water storage tower as the prototype. The parameters of the model and prototype systems are given in Table 2. The Reynolds number for the model case was 150,000. Therefore, viscous effects were insignificant. This was also verified numerically. The validity of scaling was checked numerically by re-performing the numerical solution to predict the response of the prototype system. The results obtained for the model system were duplicated identically. These results were presented in Figure 6(c) earlier. To compare the two systems, the force and displacement magnitudes were scaled using equations (2) and (6). Hence, a displacement of 1·3 mm and a force of 0·4 N for the small system would be 50 mm and 22,760 N for the large system. The suggested scaling procedure is useful for this highly non-linear system with strong fluid–oscillator and fluid–baffle plate interactions.

TABLE 2

System parameters of model and prototype absorber–structure systems

	Numerical model	Numerical prototype
Container length (mm)	130	5000
Container width (mm)	210	8100
Liquid depth (mm)	100	3800
Initial displacement (mm)	1·3	50
Reynolds number	150,000	150,000
Liquid viscosity ($N s/m^2$)	0·001	0·24
Liquid density (kg/m^3)	1020	1020
Fundamental sloshing Frequency (Hz)	2·2	0·35
Liquid mass (kg)	2·8	158,427
Structural mass (kg)	28	15,84,270
Spring stiffness (N/m)	6374	9,376,283
Structural natural frequency (Hz)	2·3	0·37
Time Step(s)	0·001	0·006

It should be mentioned here that it may not be possible practically to achieve scaling of all the non-dimensional parameters. In such cases, scaling the viscosity through the Reynolds number may be relaxed as mentioned earlier in this section.

5. CONCLUSIONS

A sloshing absorber of standing-wave type is proposed as an alternative to a tuned vibration absorber. Geometry of liquid storage tanks are more likely to have deep levels of liquid which lead to a standing-wave-type sloshing. A standing wave, on the other hand, has poor energy dissipation characteristics which make it an improper choice as a sloshing absorber. Cantilevered baffle plates are employed in this study to enhance the performance of the sloshing absorber to control the transient oscillations of a structure. A numerical procedure is described to couple the fluid solution for sloshing, with the solution of the structure to be controlled. Simple experiments were performed to verify the accuracy of the numerical predictions.

For the test geometry, 10 mm long 3 mm thick baffle plates placed 5 mm under the free surface were found to be the best configuration. Experimentally observed performance of this particular case is quite comparable to that of the optimally damped tuned absorber. In contrast to a damped tuned absorber, however, a sloshing absorber is virtually maintenance free. A procedure is presented to scale the geometry and the results.

ACKNOWLEDGMENTS

J. G. Anderson is an Australian Postgraduate Award recipient.

REFERENCES

1. J. B. HUNT 1979 *Dynamic Vibration Absorbers*. Letchworth, London: The Garden City Limited.
2. J. C. SNOWDON 1968 *Vibration and Shock in Damped Mechanical Systems*. New York: Wiley.

3. S. HAYAMA and M. IWABUCHI 1986 *Bulletin of Japanese Society of Mechanical Engineers* **29**, 1834–1841. A study on the suppression of sloshing in a liquid tank (1st Report, Suppresion of sloshing by means of a reversed U-tube).
4. K. MUTO, Y. KASAI and M. NAKAHARA 1988 *Transactions of the American Society of Mechanical Engineers, Journal of Pressure and Vessel Technology* **110**, 240–246. Experimental tests for suppression effects of water restraint plates on sloshing of a water pool.
5. F. HARA and H. SHIBATA 1987 *Japanese Society of Mechanical Engineers International Journal* **30**, 318–323. Experimental study on active suppression by gas bubble injection for earthquake induced sloshing in tanks.
6. R. SHARMA, S. E. SEMERCIGIL and Ö. F. TURAN 1992 *Journal of Sound and Vibration* **155**, 365–370. Floating and immersed plates to control sloshing in a cylindrical container at the fundamental mode.
7. J. G. ANDERSON, Ö. F. TURAN and S. E. SEMERCIGIL 1997. *The American Society of Mechanical Engineers Fluids Engineering Division Summer Meeting. Paper No.* FEDSM97-3134. Control of sloshing in rigid wall containers; Part II–A numerical approach.
8. K. FUJII, Y. TAMURA and Y. TAWAHARA 1990 *Journal of Wind Engineering and Industrial Aerodynamics* **33**, 263–272. Wind-induced vibration of tower and practical applications of tuned sloshing damper.
9. M. ABE, S. KIMURA and Y. FUJINO 1996 *3rd International Conference on Motion and Vibration Control,* 7–11. Semi-active tuned column damper with variable orifice openings.
10. V. J. MODI and F. WELT 1984 *The American Society of Mechanical Engineers Joint Multidivisional Symposium on Flow-Induced Oscillations* (Paidoussis *et al.*, editors), Vol. 1, 173–187. Nutation dampers and suppression of wind induced instabilities.
11. M. L. SETO and V. J. MODI 1997 The American Society of Mechanical Engineers *Fluids Engineering Division summer Meeting, Paper no.* FEDSM97-3302. A numerical approach to liquid sloshing dynamics and control of fluid–structure interaction instabilities.
12. S. KANEKO and O. YOSHIDA 1994 *The American Society of Mechanical Engineers, Sloshing, Fluid-Structure Interaction and Structural Response due to shock and Impact Loads, PVP-Vol.* 272, 31–42. Modelling of deep water type rectangular tuned liquid damper with submerged nets.
13. J. G. ANDERSON, S. E. SEMERCIGIL and Ö. F. TURAN 1998 *The American Society of Mechanical Engineers Fluids Engineering Division Summer Meeting, Paper No.* FEDSM98-5096, June 21–25, Washington, U.S.A. A modified sloshing absorber to control structural oscillations (to be presented).
14. S. S. RAO 1990 *Mechanical Vibration* New York: Addison-Wesley Publishing Co., second edition.
15. H. ABIRU, K. TAMURA, H. HARADA, T. MATSAMOTO and H. KONDO 1991 *Technical Review*, Vol. 28 Mitsubishi Heavy Industries Ltd. Preventing vibration in high rise structures.
16. *CFDS-FLOW3D User Guide* 1994 Computational Fluid Dynamics Services, Oxfordshire, U.K.
17. R. L. BASS, E. B. BOWLES, R. W. TRUDELL, J. NAVICKAS, J. C. PECK, N. YOSHIMURA, S. ENDO and B. F. M. POTS 1985 *Transactions of the ASME, Journal of Fluids Engineering* **107**, 272–280. Modelling criteria for scaled LNG sloshing experiments.
18. G. POPOV, S. SANKAR, T. S. SANKAR and G. H. VATISTAS 1993 *Proceedings of the Canadian Institution of Mechanical Engineers* **207**, 399–406. Dynamics of liquid sloshing in horizontal cylindrical road containers.